

Dynamics of coupled solitons in nonlinear optical fibers

Tetsuji Ueda and William L. Kath

Department of Engineering Sciences and Applied Mathematics, McCormick School of Engineering and Applied Science, Northwestern University, Evanston, Illinois 60208

(Received 15 March 1990)

A system of coupled nonlinear Schrödinger equations (NLS) governs the interaction of propagating pulses in two-mode nonlinear optical fibers and directional couplers. Using NLS solitons as trial functions in an averaged Lagrangian formulation, ordinary-differential-equation (ODE) approximations for the pulse dynamics are derived. These ODE's give a criterion for two pulses to attract one another and form a bound state; they also describe the dynamics of the complicated oscillations these pulses undergo in this bound state. In addition, the ODE dynamics show that collisions between these pulses are generally inelastic, in that there is an exchange between translational energy and internal energy (due to pulse-width oscillations). The results of the ODE theory are verified by comparison with numerical solutions of the governing partial differential equations.

I. INTRODUCTION

Propagation of distortionless pulses in polarization-preserving nonlinear optical fibers and waveguides is described by soliton solutions of the nonlinear Schrödinger (NLS) equation:

$$i \frac{\partial u}{\partial x} + \frac{1}{2} \frac{\partial^2 u}{\partial t^2} + |u|^2 u = 0.$$

Due to their distortionless propagation, it has been proposed¹ to use these solitons as information bits in long-distance optical communication systems. If the fiber or waveguide supports two distinct propagating modes, the interaction between the modes is modeled by a nonlinearly coupled system of NLS equations. When the coupling is only through instantaneous intensity overlap (as in cubic Kerr media), such a system describes the interaction of optical solitons in birefringent fibers,² directional couplers,³ and two-mode fibers.⁴ This interplay between solitons is of current interest because of the constraints it imposes on soliton-based optical communication systems. It will be shown that two spatially separated solitons, representing two distinct information bits, may attract and form a bound state or a single soliton can split apart into separate mode components, thereby leading to a degradation of transmitted data. Furthermore, it will be shown that complicated dynamics are exhibited by the two interacting solitons, in which their positions oscillate about one another and their envelope shapes deform as they propagate down the length of the fiber.

Previous investigations of coupled solitons in two-mode nonlinear fibers have used numerical simulations or analysis of the Hamiltonian formulations of the governing equations. Numerical simulations have shown the attraction and formation of bound states between two solitons and the reshaping of the pulse envelopes as the bound pulses oscillate about each other.^{5,6} However, the dynamical trajectories followed by the interacting pulses are not clear from the numerical data presented.

Analysis of the Hamiltonian has shown that the oscillations in pulse positions are periodic if the position displacements are small⁶ and has produced a potential function for pulse attraction, giving a threshold condition for two solitons to form a bound state.⁷ However, pulse envelope shapes were assumed fixed in the analysis, an assumption not verified by the numerical experiments. Furthermore, no quantitative comparisons were made between the derived soliton dynamics and true dynamics.

This paper presents analysis of interacting solitons in a nonlinearly coupled system of NLS equations using the average variational principle.⁸ Here the temporal shapes of the pulses are assumed to take a specified form but shape parameters such as pulse position and width are allowed to evolve as the pulses propagate down the fiber. With this assumption, the system of NLS equations simplifies to a reduced Lagrangian problem. By taking variations of the Lagrangian with respect to each pulse parameter, the evolution equations for the parameters are determined. By this procedure a finite-dimensional ordinary-differential-equation model of the original infinite-dimensional partial-differential-equation system is obtained, with savings in both analytical complexity and numerical computation. This variational method (as well as its Hamiltonian counterpart⁷) has been utilized previously to analyze solitons in systems of uncoupled and coupled NLS equations.⁹ Although it limits the evolution of the pulse shape to the ansatz chosen and so shape changes cannot go beyond those modeled by changes in the shape parameters, this method has been shown to give quite accurate descriptions of the evolution of perturbed NLS solitons.^{10,11} Also, this variational method gives accurate dynamics of solitons in weakly birefringent fibers.¹²

The present work presents the results of the average variational principle as well as numerical simulations of the coupled solitons to give a better understanding of their dynamics and to indicate the extent to which the Lagrangian method may be used to model such problems. It will show that, by allowing an internal degree of free-

dom in the assumed ansatz for the interacting solitons, the ordinary-differential-equation (ODE) model gives pulse dynamics which have qualitative characteristics of the true dynamics which were unobserved in previous analysis. Moreover, over a range of parameter values, quantitative accuracy of the ODE model to true dynamics is shown to be achieved. In particular, phase-plane trajectories from both the ODE model and the numerical simulations of the full partial-differential-equation (PDE) problem are plotted together which will show the quantitative accuracy achievable by this model.

II. LAGRANGIAN FORMALISM

Governing evolution equations for nonlinear optical fibers with two distinct modes operating in the anomalous group-velocity dispersion regime are given by a system of coupled NLS equations written in dimensionless form as²

$$i \left(\frac{\partial \bar{u}}{\partial x} + \delta \frac{\partial \bar{u}}{\partial t} \right) + \frac{1}{2} \frac{\partial^2 \bar{u}}{\partial t^2} + (|\bar{u}|^2 + A|\bar{v}|^2)\bar{u} = 0, \quad (1a)$$

$$i \left(\frac{\partial \bar{v}}{\partial x} - \delta \frac{\partial \bar{v}}{\partial t} \right) + \frac{1}{2} \frac{\partial^2 \bar{v}}{\partial t^2} + (|\bar{v}|^2 + A|\bar{u}|^2)\bar{v} = 0, \quad (1b)$$

where \bar{u} and \bar{v} represent the complex-valued envelopes of the two modes, t is the normalized reduced time, and x is the normalized spatial variable along the fiber length. Here, x is taken to be the evolution parameter. A is the (scaled) coefficient of the nonlinear cross-phase modulation (CPM) term and δ represents half the difference in group velocity due to linear birefringence. Using the transformations

$$\bar{u} = u \exp \left[i \frac{\delta^2}{2} x - i \delta t \right] \quad (2a)$$

$$\bar{v} = v \exp \left[i \frac{\delta^2}{2} x + i \delta t \right] \quad (2b)$$

removes the linear birefringence term from (1) and reintroduces its effect as an initial splitting velocity between the modal components of a pulse as it is injected into a birefringent fiber. This transformation gives

$$i \frac{\partial u}{\partial x} + \frac{1}{2} \frac{\partial^2 u}{\partial t^2} + (|u|^2 + A|v|^2)u = 0, \quad (3a)$$

$$i \frac{\partial v}{\partial x} + \frac{1}{2} \frac{\partial^2 v}{\partial t^2} + (|v|^2 + A|u|^2)v = 0. \quad (3b)$$

For $A \ll 1$, (3) represents two-mode fibers⁴ or directional couplers with weak intermodal coupling³ in the high-intensity limit and, for $A = \frac{2}{3}$, represents single-mode birefringent fibers² (where u and v represent the two-linear polarizations). $A = 0$ represents uncoupled NLS equations and $A = 1$ represents Manakov equations,¹³ both which admit soliton solutions as found by the inverse scattering transform method.¹⁴

A solution to (3) for exactly superimposed u - and v -mode pulses is given by

$$u = v = \eta_0 \operatorname{sech}[\sqrt{1+A} \eta_0(t - V_0 x)] \times \exp\{i \frac{1}{2}[(1+A)\eta_0^2 - V_0^2]x + iV_0 t\} \quad (4)$$

and for well-separated ($|V_1 x - V_2 x| \gg 1$) pulses or for no coupling ($A = 0$) a solution is given by

$$u = \eta_1 \operatorname{sech}[\eta_1(t - V_1 x)] \exp[i \frac{1}{2}(\eta_1^2 - V_1^2)x + iV_1 t], \quad (5a)$$

$$v = \eta_2 \operatorname{sech}[\eta_2(t - V_2 x)] \exp[i \frac{1}{2}(\eta_2^2 - V_2^2)x + iV_2 t], \quad (5b)$$

where parameters η_i and V_i represent pulse amplitudes and velocities, respectively. Both (4) and (5) correspond to the lowest-order NLS soliton. Although instabilities have been observed for cases of strong coupling or for asymmetric u and v pulses,⁵ these soliton solutions are generally stable and robust to perturbations. Since both superimposed and well-separated solutions have hyperbolic secant envelope forms, it is not unreasonable to expect that for moderate coupling strengths these sech forms are preserved for pulses with intermediate separations. So, in the present analysis, a soliton-form ansatz for the pulse shapes

$$u = \eta \operatorname{sech} \left[\frac{t-y}{W} \right] \exp i \left[V(t-y) + \frac{b}{2W}(t-y)^2 + \sigma \right] \quad (6a)$$

$$v = \bar{\eta} \operatorname{sech} \left[\frac{t-\bar{y}}{\bar{W}} \right] \exp i \left[\bar{V}(t-\bar{y}) + \frac{\bar{b}}{2\bar{W}}(t-\bar{y})^2 + \bar{\sigma} \right] \quad (6b)$$

is used, where the u -soliton shape parameters η , y , V , W , b , and σ (and their barred v -soliton counterparts) are real functions of x . The parameters η , y , and W are related to the three lowest-order moments of the u -soliton envelope and represent, respectively, its amplitude, central position, and width. The parameters σ , V , and b are related to the three lowest-order moments of the u -soliton phase; V represents the velocity of the soliton central position as it propagates along the fiber length, and b represents the frequency chirp of the soliton and is related to the change of soliton width. Frequency chirping of optical pulses has been proposed as a mechanism to achieve pulse compression.^{15,16} Barred variables in (6) have equivalent representations for the v soliton. Given this ansatz, the evolution of the soliton parameters with respect to x is determined by the averaged Lagrangian formulation (note that for $A \neq 0, 1$ the ansatz pulses are not solitons in the strict mathematical sense—they are solitonlike pulses).

The governing equations (3) restated in their Lagrangian form become^{4,6}

$$L = \int_{-\infty}^{\infty} \mathcal{L}(u, u^*, v, v^*) dt, \quad (7a)$$

where the Lagrangian \mathcal{L} is given by

$$\begin{aligned} \mathcal{L} = & i(uu_x^* - u_x u^*) + i(vv_x^* - v_x v^*) + (|u_t|^2 - |u|^4) \\ & + (|v_t|^2 - |v|^4) - 2A|u|^2|v|^2 \end{aligned} \quad (7b)$$

and (*) represents complex conjugation. Note (7a) is a function of x only since temporal forms of u and v are given (6). A system of coupled ordinary differential equations for the pulse parameters are obtained by solving the reduced variational problem

$$\delta \int L dt = 0 ,$$

taking the variation with respect to each pulse parameter.

$$\frac{\partial y}{\partial x} = V , \quad (8a)$$

$$\frac{\partial V}{\partial x} = -\frac{AK}{2W\bar{W}} \int_{-\infty}^{\infty} \text{sech}^2 \left[\frac{t-y}{\bar{W}} \right] \frac{\partial}{\partial t} \left[\text{sech}^2 \left[\frac{t-y}{W} \right] \right] dt , \quad (8b)$$

$$\frac{\partial W}{\partial x} = b , \quad (8c)$$

$$\frac{\partial b}{\partial x} = -\frac{4K}{\pi^2 W^3} \left\{ W - \frac{1}{K} + A \frac{3K\bar{W}}{2K\bar{W}} \int_{-\infty}^{\infty} \text{sech}^2 \left[\frac{t-y}{\bar{W}} \right] \frac{\partial}{\partial t} \left[(t-y) \text{sech}^2 \left[\frac{t-y}{W} \right] \right] dt \right\} , \quad (8d)$$

and the v -soliton parameters given by

$$\frac{\partial \bar{y}}{\partial x} = \bar{V} , \quad (9a)$$

$$\frac{\partial \bar{V}}{\partial x} = -\frac{AK}{2\bar{W}\bar{W}} \int_{-\infty}^{\infty} \text{sech}^2 \left[\frac{t-y}{\bar{W}} \right] \frac{\partial}{\partial t} \left[\text{sech}^2 \left[\frac{t-y}{\bar{W}} \right] \right] dt , \quad (9b)$$

$$\frac{\partial \bar{W}}{\partial x} = \bar{b} , \quad (9c)$$

$$\frac{\partial \bar{b}}{\partial x} = -\frac{4\bar{K}}{\pi^2 \bar{W}^3} \left\{ \bar{W} - \frac{1}{\bar{K}} + A \frac{3K\bar{W}}{2K\bar{W}} \int_{-\infty}^{\infty} \text{sech}^2 \left[\frac{t-y}{\bar{W}} \right] \frac{\partial}{\partial t} \left[(t-y) \text{sech}^2 \left[\frac{t-y}{\bar{W}} \right] \right] dt \right\} , \quad (9d)$$

where

$$K = \eta^2 W ,$$

$$\bar{K} = \bar{\eta}^2 \bar{W}$$

are constants of integration which arise out of the analysis. Note that these constants as well as two others,

$$\frac{V}{K} + \frac{\bar{V}}{\bar{K}} = \text{const}$$

and

$$\begin{aligned} K \left[\frac{1}{2} V^2 + \frac{\pi^2}{24} b^2 + \frac{1}{6} \left[\frac{1}{W} - K \right]^2 \right] + \bar{K} \left[\frac{1}{2} \bar{V}^2 + \frac{\pi^2}{24} \bar{b}^2 + \frac{1}{6} \left[\frac{1}{\bar{W}} - \bar{K} \right]^2 \right] \\ + \frac{A\bar{K}K}{2\bar{W}W} \int_{-\infty}^{\infty} \text{sech}^2 \left[\frac{t-y}{W} \right] \text{sech}^2 \left[\frac{t-y}{\bar{W}} \right] dt = \text{const} , \end{aligned} \quad (10)$$

are related to three lowest-order conserved quantities that the governing equations (1) obey

$$\frac{\partial}{\partial x} I^{\bar{u}} = 0 , \quad \frac{\partial}{\partial x} I^{\bar{v}} = 0 ,$$

The resulting ODE system derived by this averaged Lagrangian formalism models the original PDE system. Accuracy of this model in describing true pulse dynamics depends upon how appropriately the pulse-shape ansatz was chosen; it will be shown that, by inclusion of the chirp parameter, the ODE model gives improved trajectories as compared to those given by previous results.

III. PULSE PARAMETER EVOLUTION EQUATIONS

Solving the reduced variational problem, a coupled system of eight ODE's for the soliton parameters is obtained, with the u -soliton parameters given by

$$\frac{\partial}{\partial x} (J^{\bar{u}} + J^{\bar{v}}) = 0 ,$$

$$\frac{\partial}{\partial x} (H^{\bar{u}} + H^{\bar{v}} - H_{\text{int}}^{\bar{u}\bar{v}}) = 0 ,$$

where

$$I^\varphi = \int_{-\infty}^{\infty} |\varphi|^2 dt ,$$

$$J^\varphi = i \int_{-\infty}^{\infty} (\varphi \varphi_t^* - \varphi^* \varphi_t) dt ,$$

$$H^\varphi = \int_{-\infty}^{\infty} (|\varphi_t|^2 - |\varphi|^4) dt ,$$

$$H_{\text{int}}^{\varphi\psi} = 2A \int_{-\infty}^{\infty} |\psi|^2 |\varphi|^2 dt ,$$

which, treating solitons as classical particles,¹⁷ indicates that this system conserves individual “mass,” total “momentum” and total “energy” of interacting solitons. For the uncoupled system ($A=0$), each NLS equation separately conserves its mass (I^u, I^v), momentum (J^u, J^v), and energy (H^u, H^v) (as well as an infinite number of other conserved quantities).¹⁴ With the nonlinear coupling, although individual mass is still conserved, individual momentum need not be. Only the sum of the two momentums remains constant. $H_{\text{int}}^{\varphi\psi}$ represents the effect of the coupling on the system energy. The inclusion of the chirp parameters in the expression for the system energy allows soliton collisions to be “inelastic”—viz., energy may be transferred from the relative motions of solitons to excite internal pulse-width oscillations. More on this subject will be said later. Pulse parameters σ and $\bar{\sigma}$ drop out of the analysis since they are completely determined by the other parameters; this is due to the incoherent nature of the interaction—i.e., coupling in (3) is independent of the relative phase between u and v .

Analysis of the pulse dynamics may now proceed by solving the given ODE system. It is not possible to evaluate the integrals in (8) and (9) explicitly, however, except for some special cases. One such case is where the interacting pulses are symmetric with respect to their mean position, i.e.,

$$\begin{aligned} y &= -\bar{y}, & V &= -\bar{V}, \\ W &= \bar{W}, & b &= \bar{b}, \\ \eta &= \bar{\eta}, & K &= \bar{K}. \end{aligned} \quad (11)$$

This simplifies (8) and (9) to

$$\frac{\partial y}{\partial x} = V, \quad (12a)$$

$$\frac{\partial V}{\partial x} = \frac{2KA}{W^2} \frac{\partial}{\partial \alpha} [F(\alpha)], \quad (12b)$$

$$\frac{\partial W}{\partial x} = b, \quad (12c)$$

$$\begin{aligned} \frac{\partial b}{\partial x} &= \frac{4}{\pi^2 W^2} \left[\frac{1}{W} - K - 3AK \frac{\partial}{\partial \alpha} [\alpha F(\alpha)] \right] \\ &\equiv B(y, W; K, A), \end{aligned} \quad (12d)$$

where

$$F(\alpha) = \frac{\alpha \cosh \alpha - \sinh \alpha}{\sinh^3 \alpha},$$

$$\alpha = \frac{2y}{W},$$

and now the Hamiltonian system has two degrees of freedom in y and W . Note (y, V) and (W, b) are its conjugate pairs. This system satisfies the reduced Hamiltonian,

$$H = H_k + H_i, \quad (13)$$

where

$$H = \text{const},$$

$$H_k(y, V, W) = \frac{1}{2} V^2 - \frac{AK}{W} F\left(\frac{2y}{W}\right),$$

$$H_i(W, b) = \frac{\pi^2}{24} b^2 + \frac{1}{6} \left[K - \frac{1}{W} \right]^2.$$

H_i is a measure of the internal energy in each of the u and v solitons taken up by pulse-width oscillations and is the same as the formula for the internal energy of a perturbed NLS soliton.¹⁰ H_k is a measure of the energy in the soliton pair taken up by relative motions of their centers. More precisely, H_k is the kinetic and potential energy due to the coupling of the u and v solitons; in fact, $F(\cdot)$ is the potential function found previously for attraction between solitons where the pulse widths are assumed fixed.⁶

If frequency chirp is left out of the ansatz but the width is allowed to vary, then (12c) and (12d) are replaced by

$$B(y, W; K, A) = 0,$$

which is an implicit equation for W in terms of y . The resulting Hamiltonian system has only one degree of freedom and its trajectories are completely determined in the (y, V) phase plane. Denoting this revised reduced Hamiltonian by carets,

$$\begin{aligned} H &\rightarrow \hat{H}, \\ H_k &\rightarrow \hat{H}_k, \\ H_i &\rightarrow \hat{H}_i = \frac{1}{6} \left[K - \frac{1}{W} \right]^2, \end{aligned}$$

and analyzing for a range of \hat{H} values shows that, for $\hat{H} < 0$, pulses attract and form a bound state (y bounded for all x), wherein the pulse central positions and widths undergo periodic oscillations. Since the widths W are completely determined by the central positions y , they both oscillate with the same period. For $\hat{H} > 0$, the pulse pair has large enough initial separation velocity to overcome the CPM-induced attraction. As $x \rightarrow \infty$, such pulses “escape” and become well-separated solitons (5). $\hat{H} = 0$ gives the threshold between these two behaviors. At this threshold, V in the revised Hamiltonian gives the “escape velocity” V_e for two initially superimposed ($y=0$) solitons,

$$V_e^2 = \frac{2}{3} K^2 A \left[1 + \frac{A}{2} \right]. \quad (14)$$

In the (y, V) phase plane, $\hat{H} = 0$ gives the separatrix which separates the regions of bound and escaping soli-

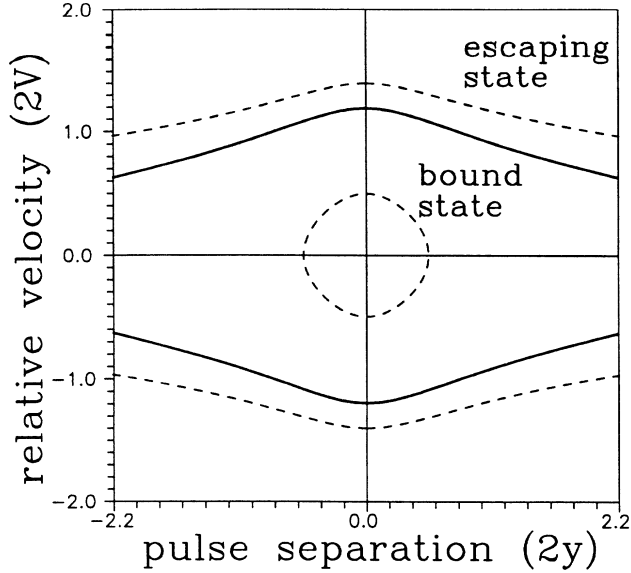


FIG. 1. Regions of bound and escaping solitons in the (y, V) phase plane from the no-chirp analysis, for initial conditions as in (15) with $\eta_0=1$ and $A=\frac{2}{3}$. (—) is the separatrix and (---) are sample bound and escaping orbits.

ton behaviors (Fig. 1). Although this no-chirp analysis gives the two different soliton behaviors of interest, it will be shown that, for the ODE model to correspond qualitatively to true pulse dynamics, the frequency chirp must be included.

Given the system (12), analysis will be carried out for two cases—(i) when the interacting solitons form a bound state; (ii) when the solitons escape. For initial conditions zero separation, arbitrary initial velocities, zero chirps, and pulse widths normalized to the exact superimposed soliton solution, i.e.,

$$y=0, \quad V=V_0=\delta, \quad (15)$$

$$\eta=\eta_0, \quad W=\frac{1}{\eta_0\sqrt{1+A}},$$

$$b=0, \quad \sigma=0$$

for $x=0$, will be used. These initial conditions model a soliton injected into a fiber with polarization at 45° to the fast and slow axes.

A. Bound-state solitons

For superimposed u and v solitons with initial separation velocity not large enough to overcome mutual attraction due to CPM, the pulses trap each other and form a bound state. In this state, their widths oscillate and their central positions oscillate. The centers oscillate about a mean position which propagates with the average of their linear group velocities. Numerical simulations of the governing equations (3) show such oscillations (Fig. 2). Detailed measurements of the numerical data suggests that these pulse position and width oscillations are not commensurate and that these oscillations are not

periodic. Previous analyses, where the widths were assumed fixed, and the no-chirp analysis give results which do not correspond to these qualitative dynamical behaviors.

In comparison to these analyses, the better qualitative agreement of the chirped ODE model (12) to true pulse dynamics is seen in Fig. 3, where the (y, V) phase-plane trajectories given by the model are plotted along with the results of no-chirp analysis and the true dynamics as computed by numerical simulations of the full PDE. Since the inclusion of chirp in the ODE model allows an extra degree of freedom, the resulting trajectories, unlike in the no-chirp analysis, do not close and are quasiperiodic, and the pulse position and width oscillations are not commensurate. This is because the kinetic and internal oscillations in this model are governed by different characteristic frequencies. Taking H_k and H_i to be independent of each other and scaling H_k near $y \sim 0$ (with W held constant) and scaling H_i near $W \sim 1/K$ (with no coupling $A=0$), equations describing periodic motions can be derived with frequencies given by

$$\omega_k^2 = \frac{16}{15} \frac{AK}{W^3},$$

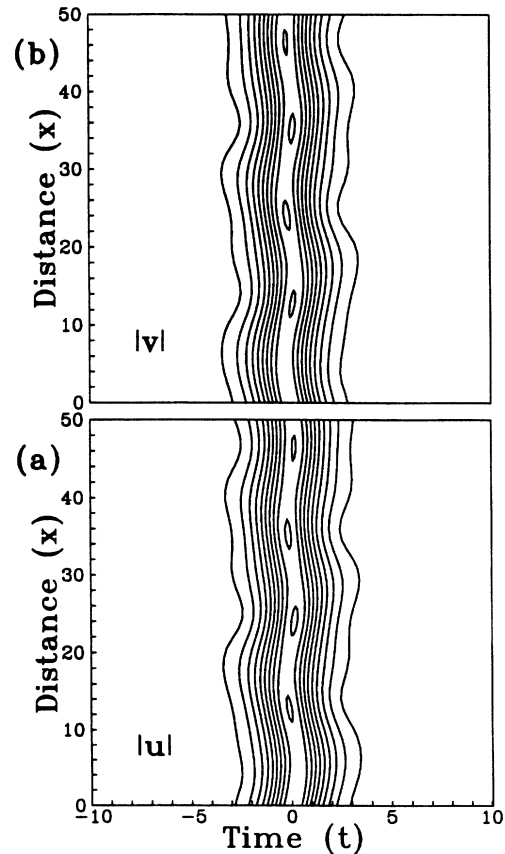


FIG. 2. Contour plots of (a) $|u|$ and (b) $|v|$ showing motion of coupled solitons, for initial conditions as in (15) with $V_0=0.2$, $\eta_0=1$, and $A=0.1$. Contours are evenly spaced between 0.1–1.0.

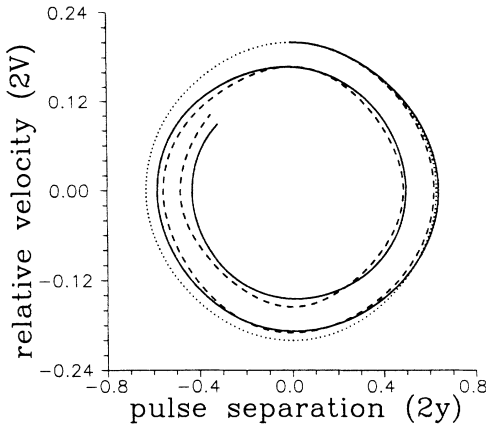


FIG. 3. Comparisons of true and model trajectories in the (y, V) phase plane for initial conditions as in Fig. 2. (—) true (computed), (- - -) ODE model (12), and (· · ·) no-chirp model.

$$\omega_i^2 = \frac{4}{\pi^2} K^4.$$

This additional degree of freedom in the ODE model allows collisions of the interacting solitons to be “inelastic,” in which their widths may stretch in response to the CPM-induced attraction. The reduced Hamiltonian indicates that there is a transfer of energy between H_k and H_i (Fig. 4). Since $H_i \geq 0$, internal oscillation excitation would, for equal values of the reduced Hamiltonian constant H , decrease the allowable pulse velocities and separation from the case where no such oscillations are permitted. Although the previous fixed-width analysis does not give accurate pulse trajectories, it does provide maximum separation and velocity values for interacting solitons. Using the solitons-as-particles analogy, the inelastic nature of the soliton collisions is explained by this

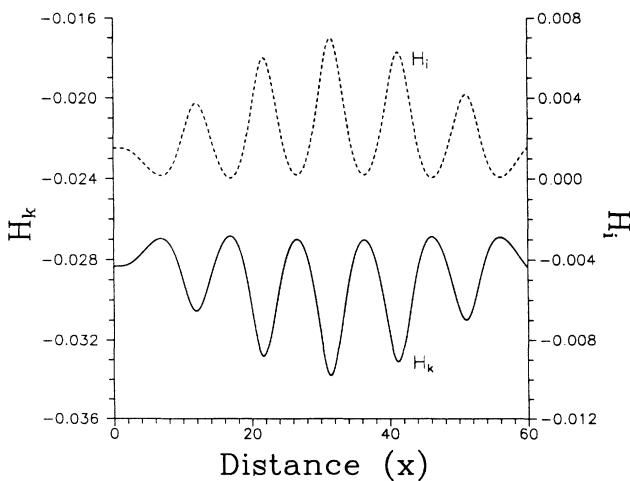


FIG. 4. Exchange of energies between H_k and H_i for bound-state solitons as the pulses evolve in x . Initial conditions as for Fig. 2. (—) H_k and (- - -) H_i .

transference of energy—since internal oscillations are excited with each soliton-soliton collision, the back-and-forth motions of the solitons are reduced from those predicted by previous elastic results.

In addition to the improved qualitative agreement, Fig. 3 shows the better quantitative accuracy of the chirped ODE model in following the true soliton trajectory. Due to the use of NLS solitons as the pulse-form ansatz, accuracy of trajectories from the ODE model is best for small A (weak CPM) and small separation between the solitons—i.e., when the interacting solitons remain close to the exactly superimposed soliton solution (4). For small A the weak CPM diminishes the degree of the asymmetric reshaping of pulse tails caused by uneven nonlinear coupling when the pulses only partially overlap. This asymmetry has been seen in previous numerical computations.⁵ For such asymmetric effects to be analyzed in the averaged Lagrangian formalism, higher-order moments of the pulse envelopes would need to be included in the ansatz (6). Small separation of bound-state solitons prevents the significant reshaping of the soliton envelope shapes which occur for pulses which separate far enough such that their envelopes oscillate between the superimposed soliton form (4) and the well-separated soliton form (5). Such large envelope reshaping leads to the emission of significant amounts of linearly

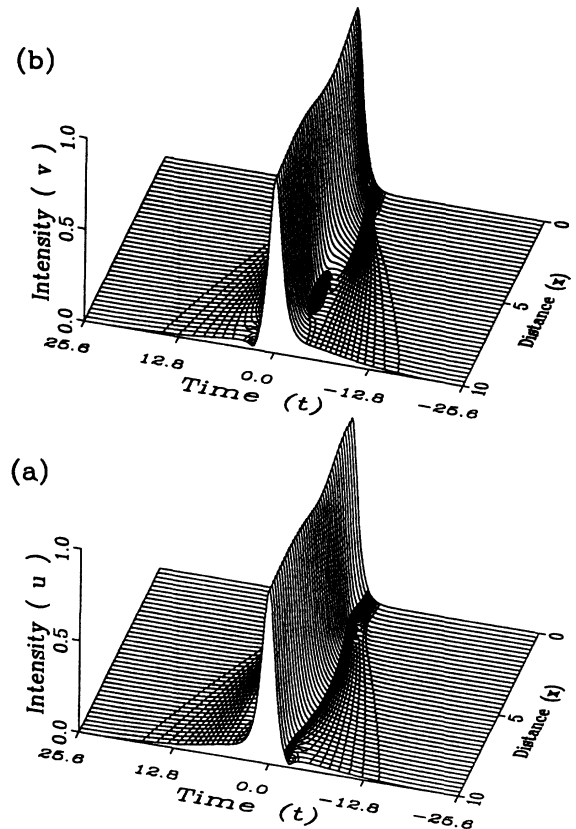


FIG. 5. Intensity plots of (a) $|u|$ and (b) $|v|$ showing low-wave-number radiation shelf emitted from coupled solitons, for initial conditions (15) with $V_0=0.6$, $\eta_0=1$, and $A=\frac{2}{3}$. Plot rotated to show end profile.

dispersive radiation from the pulses, a process which is analogous to the production of continuous spectrum modes in perturbed NLS solitons.¹⁸ This radiation disrupts pulse dynamics by interacting directly with the solitons and by carrying energy away from the pulses. Figure 4 shows that the ODE model feeds internal energy back into the nonlinear kinetic oscillations, while in the original governing PDE some internal energy is fed to the radiating modes and is lost. This appears to be one of the reasons that the two trajectories in Fig. 2 diverge, with the oscillations of the true dynamics becoming smaller than the oscillations given by the ODE model.

It has been shown that this radiation affects the dynamics of adjacent solitons over long distances in a communication line,¹⁹ and so is not a desirable by-product of pulse interaction. In particular, pulse dynamics are sensitive to low-wave-number radiation which is observed numerically as a low “shelf” at the tails of the interacting pulses (Fig. 5). Such radiation propagates at velocities close to that of the solitons and remains close to the pulses and affects their dynamics over long time scales.²⁰

Nevertheless, the ODE model as is still gives a better understanding of how CPM coupling of two solitons excite mutual and internal oscillations and gives quantitative accuracy of true pulse dynamics for pulses close to the exact soliton solutions of (3), with savings in both analytical and numerical complexity. How to appropriately include higher-order momentum and radiation in the pulse-form ansatz is the subject of current work.

B. Escaping solitons

For superimposed u and v solitons with initial splitting speed fast enough to overcome mutual attraction due to CPM, the solitons escape and become well-separated solutions (5) as $x \rightarrow \infty$ (plus any emitted radiation). When the pulse widths are assumed fixed, a threshold for solitons to escape has been derived, giving a separatrix in the phase plane dividing the regions of escaping and bound states. For initially overlapping pulses, this threshold gives a minimum splitting speed, or “escape velocity,” for two interacting solitons. From (13), using the same arguments as for the bound-state solitons, for initially unchirped pulses, the loss of initial kinetic energy into the excitation of internal width oscillations effectively increases the escape velocity from that given by the previous analysis. This suggests that it is not just the detuning of the soliton central frequencies² which stabilize coupled solitons against escaping, but that changes in higher-order moments of the soliton phases also contribute to the stabilization. To obtain this improved escape threshold, the ODE system (12) must be solved. The change in the escape velocity for certain values of A is given in Table I. It is seen that this change is greater for larger values of A . Numerical simulations of the governing equations support the larger escape velocities obtained from the ODE model.

Conversely, if instead of initial conditions (15) pulses have initial chirp $b \neq 0$, then the transfer of energy from internal to kinetic motions can cause a decrease in the initial velocity necessary for escape. Thus the presence of

TABLE I. Escape velocity V_e for given values of A from no-chirp (14) and chirped (12) analyses.

A	Escape velocity V_e	
	no-chirp	chirped
0.1	0.252	~ 0.26
$\frac{2}{3}$	0.596	~ 0.75

frequency chirping in solitons injected into a birefringent fiber may destabilize the bound state.

For the case of escaping solitons, the transfer of energy between H_k and H_i as the pulses evolve in x may be seen in Fig. 6. After an initial period of exchange, H_k and H_i both approach constant values as $x \rightarrow \infty$. This quantifies the obvious fact that the two processes, one for the kinematic pulse-center motions and the other for the internal pulse-width changes, effectively decouple for escaping solitons. The length of x for which H_k and H_i undergo significant changes may be considered the “interaction length” for the two interacting solitons.

Analysis of the ODE model (12) suggests two possible types of behaviors for escaping solitons. In one behavior, occurring when the splitting velocity is large compared to the escape velocity, widths of the escaping solitons oscillate due to the excitation of internal oscillations and the solitons become, in effect, perturbed NLS solitons.¹⁸ In the other, occurring where the splitting velocity is close to the escape velocity, width increases linearly in x as $x \rightarrow \infty$ but at the same rate as y increases (i.e., $\alpha \approx \text{const}$). The latter case is of interest since, in the limit $x \rightarrow \infty$, the interacting solitons should decay, with pulse amplitude $\eta \sim 1/\sqrt{x}$, until they completely break apart into linearly dispersive radiation. Linearly dispersing pulse solutions, which are the asymptotic limits of this case, have been

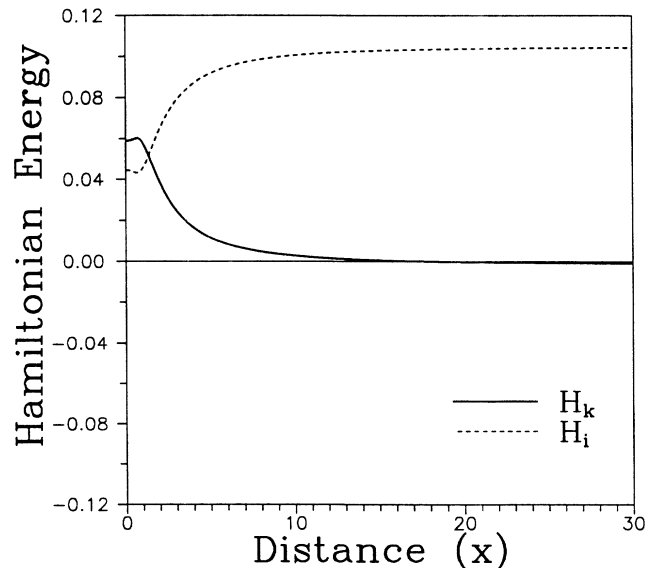


FIG. 6. Exchange of energies between H_k and H_i for escaping solitons as the pulses evolve in x . Initial conditions (15) with $V_0 = 1.5$, $\eta_0 = 1$, and $A = \frac{2}{3}$. (—) H_k and (---) H_i .

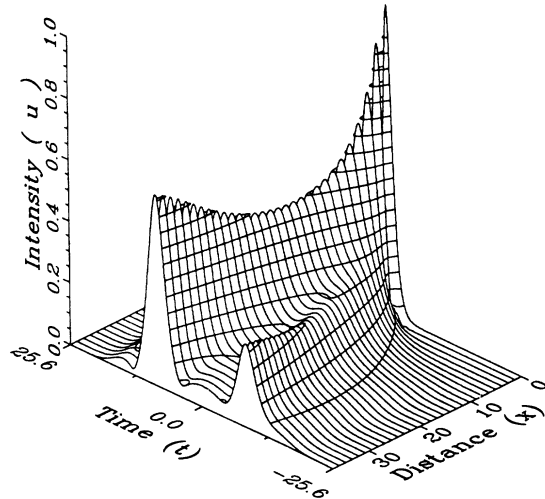


FIG. 7. Intensity plot of $|u|$ showing shadow solitons, for initial conditions (15) with $V_0=0.75$ (near threshold), $\eta_0=1$, and $A=\frac{2}{3}$. Plot rotated to show end profile. The $|v|$ envelope is mirror symmetric with the $|u|$ envelope about $t=0$.

analyzed previously for the uncoupled NLS system.¹⁰ However, this escape behavior could not be replicated in numerical simulations of the coupled NLS. Numerics do suggest, however, that the linearly increasing widths herald the formation of shadow pulses,² small daughter pulses which split off from a soliton in one mode to propagate alongside or “shadow” the soliton in the other mode (Fig. 7). The width increase and the accompanying longer soliton interaction time predicted by the ODE theory may allow local nonlinear CPM effects to invalidate the single NLS soliton assumption used in the ansatz.

Numerical simulations show that the process of escape is noisy in that appreciable radiation is emitted from the separating solitons. As mentioned earlier, the possibility of including radiation in the ansatz (6) is the subject of current work.

IV. SUMMARY AND CONCLUSIONS

An averaged variational principle using NLS solitons with varying parameters as an ansatz has been used to analyze the soliton-soliton interactions in a system of nonlinearly coupled NLS equations. The parameters chosen are essentially the lowest-order moments of the soliton envelopes and phases. The variational principle gives a straightforward method to determine the evolution of the pulse parameters which are considered to be of significance and reduces the original infinite-dimensional PDE system for the pulse waveforms to a finite-dimensional ODE system for the pulse parameters. It has been shown that the inclusion of frequency chirping and width variations and the additional internal degree of freedom it gives in the resulting Hamiltonian system causes soliton-soliton collisions to be inelastic. Furthermore, it has been shown that their inclusion allows energy to be exchanged between the kinetic pulse-center motions and the internal pulse-width oscillations. When the solitons form a bound state, this causes soliton dynamics to lie on quasiperiodic orbits. When the two solitons escape, this causes an increase in the threshold escape velocity and acts to stabilize the bound state for a given value of Hamiltonian energy. Moreover, greatly improved quantitative accuracy in predicting soliton dynamics compared to previous ODE models is achieved. This work also shows that to obtain models with an even higher degree of approximation to the true pulse dynamics, the effects of higher-order envelope moments and radiation, which draws energy from internal oscillations and away from the solitons, must be included in the pulse-shape ansatz. This is the subject of current research.

ACKNOWLEDGMENTS

The authors would like to thank Professor Alejandro B. Aceves for helpful discussions initial to this work, and David J. Muraki for many valuable discussions throughout the course of this work and for providing his numerical routines. This research was supported in part by grants from the National Science Foundation (Applied Mathematics, Grant No. 8451768 and Scientific Computing Research Equipment Grant No. 8905616) and by a grant from the Air Force Office of Scientific Research (Mathematical Sciences, Grant No. 85-0150).

¹A. Hasegawa and F. Tappert, *Appl. Phys. Lett.* **23**, 142 (1973).
²C. R. Menyuk, *IEEE J. Quantum Electron.* **QE-23**, 174 (1987); *Opt. Lett.* **12**, 614 (1987); *IEEE J. Quantum Electron.* **QE-25**, 2674 (1989).
³S. M. Jensen, *IEEE J. Quantum Electron.* **QE-18**, 1580 (1982); Y. Silberberg and G. I. Stegeman, *Appl. Phys. Lett.* **50**, 801 (1987).
⁴B. Crosignani and P. Di Porto, *Opt. Lett.* **6**, 329 (1981).
⁵E. M. Wright, G. I. Stegeman, and S. Wabnitz, *Phys. Rev. A* **40**, 4455 (1989); C. R. Menyuk, *Opt. Lett.* **12**, 614 (1987); *J. Opt. Soc. Am. B* **5**, 392 (1988).
⁶V. V. Afanasyev, Yu. S. Kivshar, V. V. Konotop, and V. N. Serkin, *Opt. Lett.* **14**, 805 (1989).
⁷E. Caglioti, B. Crosignani, and P. Di Porto, *Phys. Rev. A* **38**,

4036 (1988).

⁸G. B. Whitham, *Linear and Nonlinear Waves* (Wiley-Interscience, New York, 1974).

⁹D. Anderson, *Phys. Rev. A* **27**, 3135 (1983); D. Anderson and M. Lisak, *ibid.* **32**, 2270 (1985); *Opt. Lett.* **11**, 174 (1986).

¹⁰D. Anderson, M. Lisak, and T. Reichel, *J. Opt. Soc. Am. B* **5**, 207 (1988).

¹¹D. Anderson, M. Lisak, and T. Reichel, *Phys. Rev. A* **38**, 1618 (1988); M. Desaix, D. Anderson, and M. Lisak, *ibid.* **40**, 2441 (1989).

¹²D. J. Muraki (private communication).

¹³S. V. Manakov, *Zh. Eksp. Teor. Fiz.* **65**, 505 (1973) [*Sov. Phys.—JETP* **38**, 248 (1974)].

¹⁴A. C. Newell, *Solitons in Mathematics and Physics* (Society for

- Industrial and Applied Mathematics, Philadelphia, 1985).
- ¹⁵D. Grischkowsky and A. C. Balant, *Appl. Phys. Lett.* **41**, 1 (1982).
- ¹⁶G. P. Agrawal, P. L. Baldeck, and R. R. Alfano, *Phys. Rev. A* **40**, 5063 (1989).
- ¹⁷D. J. Kaup and A. C. Newell, *Proc. R. Soc. London Ser. A* **361**, 413 (1978).
- ¹⁸J. Satsuma and N. Yajima, *Prog. Theor. Phys.* **55**, 284 (1974).
- ¹⁹K. Smith and L. F. Mollenauer, *Opt. Lett.* **14**, 1284 (1989).
- ²⁰L. F. Mollenauer, K. Smith, J. P. Gordon, and C. R. Menyuk, *Opt. Lett.* **14**, 1219 (1989).